Grain Size Dependence of Dynamic Strain Ageing During Low Cycle Fatigue in Type 304 Stainless Steel

K. BHANU SANKARA RAO, M. VALSAN, R. SANDHYA, S. L. MANNAN and P. RODRIGUEZ

Metallurgy Programme, Indira Gandhi Centre for Atomic Research, Kalpakkam, 603 102, India

ABSTRACT

The grain size (GS) dependence of dynamic strain ageing (DSA) and its influence on low cycle fatigue (LCF) life, deformation and fracture behaviour of type 304 stainless steel has been investigated at 823K, employing the cyclic deformation rates from 1.6×10^{-4} to 1.6×10^{-2} s^{-1}. A total strain range of 0.8% is used for all the tests. Grain sizes studied include 75, 310 and 700 μm. All the grain sizes show loss of fatigue life with reduction in strain rate ($\dot{\epsilon}$) due to DSA effects. Medium GS is more affected by DSA. DSA in LCF is manifested as a peak in the saturation stress, a minimum in plastic strain, increased work hardening rate and is at times associated with serrated stress-strain hysteresis loops. The fracture mechanisms and fatigue life are influenced to a great extent by prevailing deformation mechanisms. The inhomogenity of deformation results from DSA effects during LCF. Intense slip bands are observed in the interior of medium and coarse grained material. The impingement of these slip bands on grain boundaries caused brittle intergranular decohesion. TEM and SEM observations are presented to explain the variations in fatigue life as a function of GS and $\dot{\epsilon}$.

KEYWORDS

Low cycle fatigue; grain size; dynamic strain ageing; type 304 stainless steel; deformation; fracture.

INTRODUCTION

At elevated temperatures the decrease in fatigue life with decreasing strain rate ($\dot{\epsilon}$) or increasing test temperature has been considered to be due to creep damage or to be an environmental effect such as oxidation (Coffin Jr, 1973; Bhanu Sankara Rao et al., 1986a; Bhanu Sankara Rao et al., 1988a). Studies on austenitic stainless steels (Yamaguchi et al., 1978; Bhanu Sankara Rao et al., 1986b; Bhanu Sankara Rao, 1988b) have indicated that the life reduction with decreasing $\dot{\epsilon}$ can also occur in the sub-creep

temperature regime due to deleterious effects of dynamic strain ageing (DSA). The results on austenitic stainless steels strongly suggest that for the LCF life at elevated temperatures, the effect of DSA should be considered in addition to the environment effect and creep damage. The present investigation deals with the effects of GS and $\dot{\epsilon}$ on the cyclic deformation and fracture behaviour of type 304 stainless steel at 823K.

EXPERIMENTAL DETAILS

The material examined has its chemical composition (in wt%) 18.2Cr, 9.2Ni, 0.042C, 0.38Si, 1.65Mn, 0.024P, 0.003S and balance Fe. The heat treatments employed, the resulting average grain sizes and the tensile properties of three different grain sizes at 823K are given in Table 1. Fully reversed total axial strain controlled LCF tests were conducted on 25 mm gauge length, 10 mm dia cylindrical ridge samples in an Instron 1343 servohydraulic system equipped with radiant heating facility. Tests were carried out at 823K using a triangular wave form over a frequency (ν) range of 10^{-2} to 1.0 Hz, at a strain range ($\Delta\epsilon_t$) of 0.8%. Fracture surfaces of the failed specimens were examined in a Philips PSEM 501 scanning electron microscope, while TEM investigations of thin foils prepared from slices taken over the gauge section of fractured samples were conducted on Philips EM 400 operating at 100 keV. In this investigation, the number of cycles corresponding to the 20% drop in maximum stress in tension is reported as the fatigue life, N_f.

Table 1. Heat treatments employed in generating different grain sizes, and tensile properties at 823K for $\dot{\epsilon} = 3.0 \times 10^{-4}\ s^{-1}$

Heat treatment	Grain Size (μm)	0.2% YS (MPa)	UTS (MPa)	El (%)	RA (%)
1323 K/1/2 h, Water Quench (WQ)	75	136	402	43.0	70.8
1573 K/1/2 h, WQ + 1323 K/1/2 h, WQ	310	108	336	32.5	78.2
1623 K/1/2 h, WQ + 1323 K/1/2 h, WQ	700	107	336	38.5	78.8

RESULTS AND DISCUSSION

Influence of Grain Size and Strain Rate on LCF Properties

Table-2 summarizes the combined influence of GS and $\dot{\epsilon}$ on LCF properties such as number of cycles to failure N_f, number of cycles to macro-crack initiation N_I, number of cycles spent in propagation N_p, tensile stress amplitude in the first cycle $(\Delta\sigma/2)_1$, maximum tensile stress amplitude $(\Delta\sigma/2)_{max}$ and the plastic strain range ($\Delta\epsilon_p$) per cycle at $(\Delta\sigma/2)_{max}$. N_f decreases markedly with decreasing $\dot{\epsilon}$ in case of medium (310 μm) and coarse (700 μm) GS. Fine (75 μm) GS exhibits a peak in N_f at

Table 2. Low cycle fatigue properties as a function of grain size and $\dot{\epsilon}$ at 823K ($\Delta\epsilon_t = 0.8\%$)

Grain size (μm)	$\dot{\epsilon}$ (s^{-1})	$\Delta\epsilon_p$ (%)	$(\frac{\Delta\sigma}{2})_1$ (MPa)	$(\frac{\Delta\sigma}{2})_{max}$ (MPa)	N_I	N_p	N_f	Remarks
75	1.6×10^{-2}	0.569	183	238	900	169	1069	O
75	1.6×10^{-3}	0.480	159	271	800	490	1290	◒
75	1.6×10^{-4}	0.424	138	279	550	246	796	●
310	1.6×10^{-2}	0.567	159	227	600	1790	2390	O
310	1.6×10^{-3}	0.562	147	262	160	555	715	◒
310	1.6×10^{-4}	0.555	112	271	220	209	429	●
700	1.6×10^{-2}	0.500	113	232	550	2450	3000	O
700	1.6×10^{-3}	0.412	102	255	500	775	1275	◒
700	1.6×10^{-4}	0.368	108	278	450	375	875	●

O Smooth stress-strain hysteresis loops. ◒ smooth stress-strain hysteresis loops + dynamic strain ageing. ● Serrated flow in the plastic regions of stress-strain hysteresis loops.

the intermediate $\dot{\epsilon}$. Medium and coarse GS show higher N_f at higher $\dot{\epsilon}$ than fine GS while minimum N_f is recorded for medium GS at the two lower strain rates. All the grain sizes display markedly unstable plastic flow in the plastic regions of stress-strain hysteresis loops at the lowest $\dot{\epsilon}$ employed (Fig.1).

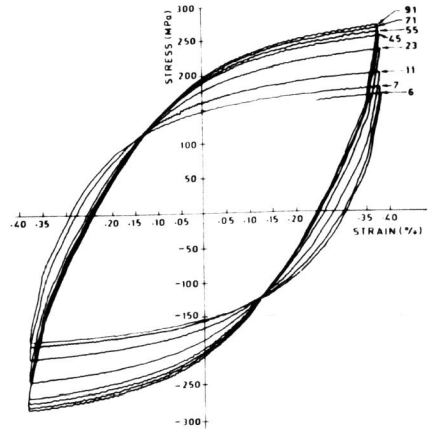

Fig. 1. Hysteresis loops showing serrated flow (GS = 75 μm, $\dot{\epsilon} = 1.6 \times 10^{-4}\ s^{-1}$).

A summary of the tensile stress response derived from the hysteresis loops recorded for different strain rates is shown in Figs.2 and 3 for fine and medium GS where all tensile peak stresses of successive cycles have been normalised with respect to peak tensile stress of the first cycle. Coarse GS exhibits similar stress response as medium GS at all $\dot{\epsilon}$. The important conclusions from Figs.2 and 3 are (i) The cyclic deformation stress response is GS and $\dot{\epsilon}$ dependent. (ii) Fine GS exhibits a period of strain hardening followed by a long period of a nearly saturation stress response at all the $\dot{\epsilon}$, while medium and coarse GS show this behaviour only at higher $\dot{\epsilon}$. (iii) At the intermediate and lower $\dot{\epsilon}$, the period of strain hardening dominates the stress response for medium and coarse GS. (iv) The number of cycles required to attain the $(\Delta\sigma/2)_{max}$ increased with decreasing $\dot{\epsilon}$. (v) All the grain sizes display almost equal $(\Delta\sigma/2)_{max}$ at lower $\dot{\epsilon}$, in spite of large differences in the first cycle (vi) The large normalised cyclic hardening at the lower $\dot{\epsilon}$ and the $\dot{\epsilon}$ dependence of $(\Delta\sigma/2)_{max}$ indicates the negative strain rate sensitivity.

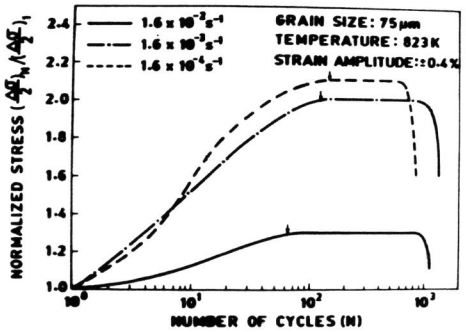

Fig. 2. Normalised stress response curves illustrating the influence of strain rate (GS = 75 μm).

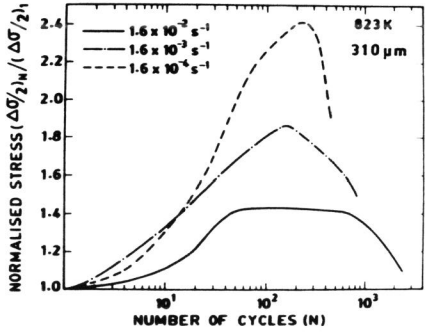

Fig. 3. Normalised stress response curves illustrating the influence of strain rate (GS = 310 μm).

The serrated flow in stress-strain hysteresis loops, the decrease in plastic strain per cycle with decreasing $\dot{\epsilon}$, the negative $\dot{\epsilon}$ sensitivity of the cyclic hardening and the associated decrease in N_f at the sub-creep temperatures are the manifestations of DSA effects in LCF (Bhanu Sankara Rao et al., 1986b; Bhanu Sankara Rao, 1988b). In spite of an increase in cyclic stress when $\dot{\epsilon}$ was changed from 1.6×10^{-2} to $1.6 \times 10^{-3} s^{-1}$, the hysteresis loops remain smooth at $\dot{\epsilon} = 1.6 \times 10^{-3} s^{-1}$ (Table-2) for all the grain sizes. This result indiates that DSA commenced earlier than it is manifested in the form of serrated flow in the stress-strain hysteresis loops.

The sharp drop of normalised tensile stress (Figs.2 and 3) before failure corresponds to a progressive reduction in the load bearing area of the specimen due to crack growth. The cycle number at which this stress drop begins may thus be used as an estimate of N_i; the number of cycles required to initiate a macroscopic crack. The results presented in Table-2 suggest that number of cycles to both crack initiation and cycles spent in propagation get affected as the $\dot{\epsilon}$ is lowered due to DSA effects. Under strong DSA conditions ($\dot{\epsilon} = 1.6 \times 10^{-4} s^{-1}$), cyclic deformation develops higher stress response leading to large stress concentration at the crack tip, which accounts for increased crack growth rate (Table-2). Higher stresses also reduce the critical crack size for final fracture, reducing N_f (Bressers and Verheghe, 1981). Significant differences in N_f at $\dot{\epsilon} = 1.6 \times 10^{-2} s^{-1}$ (Table-2) between fine GS and medium or coarse GS may be explained by considering the initiation and propagation stages. Improved fatigue resistance of medium or coarse grain sizes could be attributed to the longer macrocrack propagation stage, inspite of the fact that life for crack initiation is shorter. Intense slip bands, which are later the sites for crack nucleation at the surface, occur early in the large grained material. It is believed that a large grain allows a greater amount of reversible slip and thus, reduces the amount of accumulated plastic strain within the reverse plastic zone, enabling the reduction in crack growth.

Observations on Deformation and Fracture Behaviour

TEM studies reveal that the deformation mechanism and corresponding dislocation microstructures depend both on the GS and $\dot{\epsilon}$. The fine GS shows more uniformly distributed dense dislocation sub-structure at high $\dot{\epsilon}$ (Fig.4). Lowering the $\dot{\epsilon}$ further increased the number density of dislocations and tangles. In contrast to the more homogeneous deformation shown by fine GS at all the $\dot{\epsilon}$, medium and coarse grain sizes undergo more intense deformation in planar slip bands. The density of slip bands increases with decreasing $\dot{\epsilon}$. An important feature is that at the lower $\dot{\epsilon}$, the regions between the slip bands contained uniform distribution of dislocations (Fig.5).

At $\dot{\epsilon} = 1.6 \times 10^{-2}$ and $1.6 \times 10^{-3} s^{-1}$, the fatigue crack propagated transgranularly by the ductile striation mechanism (Fig.6a). Coincident with the large reductions in N_f, at the lower $\dot{\epsilon}$, all the grain sizes display mixed transgranular and intergranular mode of fracture (Fig.6b). However, there exist differences in the degree of intergranular cracking depending on GS. It should be pointed out that the occurrence of serrated flow coincides with the formation of intergranular cracking. In the event where negative strain rate sensitivity exists and no serrated flow occurs crack propagation remains transgranular.

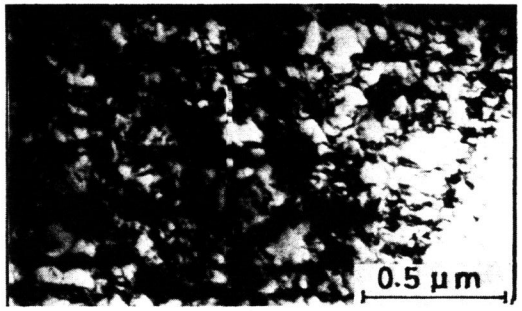

Fig. 4. Dislocation substructure in fine grained sample ($\dot{\epsilon} = 1.6 \times 10^{-2} s^{-1}$).

Fig. 5. Slip bands and uniform distribution of dislocations in the interband regions (GS = 310 µm, $\dot{\epsilon} = 1.6 \times 10^{-4} s^{-1}$).

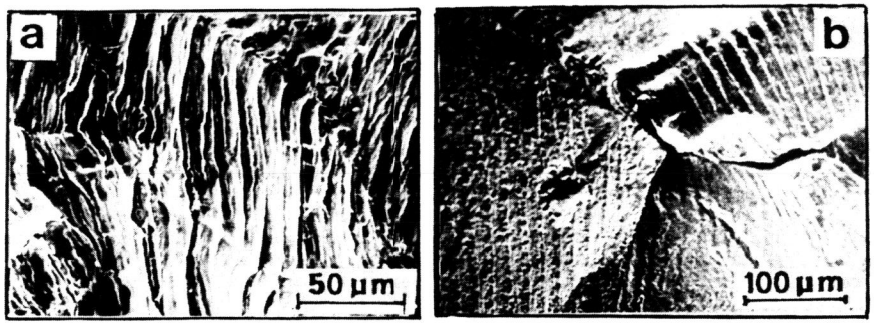

Fig. 6. (a) Transgranular propagation ($\dot{\epsilon} = 1.6 \times 10^{-3} s^{-1}$) and (b) mixed mode propagation ($\dot{\epsilon} = 1.6 \times 10^{-4} s^{-1}$). GS= 310µm.

Mechanisms of Deformation and Fracture due to DSA

From TEM studies, it is clear that conditions that cause DSA promote the formation of relatively high dislocation densities during cyclic deformation. The abnormally high rate of cyclic hardening observed in lower $\dot{\epsilon}$ tests could be associated with the increased rates of dislocation storage due to DSA. At the temperature employed in this study, DSA during tensile deformation has been considered to result from locking of mobile dislocations by substitutional solute atoms (Bhanu Sankara Rao, 1988b). Increased amount of dislocation storage and solute locking of dislocations could be invoked to explain the stronger effect of DSA on $(\Delta\sigma/2)_{max}$ than on $(\Delta\sigma/2)_f$ (see Table-2) because it is the strain hardening process which is affected to a greater extent by dislocation generation and immobilization. It may be mentioned that DSA would enhance the inhomogeneity of deformation during LCF due to solute locking of the slow moving dislocations between the slip bands (Fig.5). Presumably, the dislocation velocities maintained within the intense slip bands (Fig.5) are too high for solute - dislocation interactions to occur (Wilson and Tromans, 1970) and consequently, DSA enhances partitioning of cyclic strains into separate regions characterized by high and low amplitudes of dislocaltion movement (Abdel-Raouf et al, 1973) This phenomenon is pronounced markedly in the medium and coarse GS covered in this investigation and accompanied by loss of fatigue life.

Under DSA conditions, for medium GS, impingement of slip bands on grain boundaries causes intergranular brittle decohesion (Fig.6b). Slip bands also appear to have been cracked (Fig.6b). It is proposed that disloations moving at higher velocity in specific slip planes lead to formation of pile-ups and consequent development of back stresses. Interaction of back stresses with crack tip stresses might lead to slip band cracks (Hua et al, 1983) (Fig.6b). Intergranular decohesion due to intersection of slip bands with grain boundaries stems from the long range stresses associated with the piling up of dislocations (Mughrabi et al, 1983). The combined action of crack tip stress field and the stress concentration at the front of pile-up leads to intergranular cracking. Reduction in N_f occurs due to accelerated propagation in the event of intergranular cracking. The higher fatigue resistance of fine GS compared to medium GS under DSA condition results from the reduced incidence of intergranular cracking. Since the slip length cannot exceed the grain diameter, fine grain reduces the stress concentrations and associated intergranular cracking, by reducing the number of dislocations in a pile-up (Starke Jr, 1979). Homogeneous deformation observed under DSA conditions in fine grained material can be invoked to explain the reduced incidence of intergranular cracking and improved resistance to fatigue. It must be pointed out that coarse grain also exhibits higher resistance to fatigue than the medium GS under DSA conditions. Microscopic investigations show that many of the slip bands do not run across the coarse grain and instead get terminated abruptly in the intergranular regions. This happens because of slip lengths of very large magnitude are difficult to develop. Under such conditions the incidence of intergranular cracking decreases. Further the plastic strain developed in a cycle in coarse grained material under DSA conditions is rather small, therefore, a larger number of cycles would be needed to exhaust the ductility of the material. The fatigue life under DSA conditions do not strictly correspond to the rank order of tensile ductility exhibited by different grain sizes (Table-1).

CONCLUSIONS

1. In 304 SS, at 823K, fatigue life is dependent on grain size and $\dot{\epsilon}$. Though the temperature is in the sub-creep regime, fatigue life decreases with decreasing $\dot{\epsilon}$ due to DSA effects.
2. For all the grain sizes, maximum cyclic tensile stress response increases considerably under the influence of DSA, and stress response dependency on $\dot{\epsilon}$ is negative.
3. DSA commences earlier than it is manifested in the form of serrations in cyclic stress-strain hysteresis loops. DSA accompanied by serrated flow, leads to a drastic reduction in fatigue life.
4. DSA effects on LCF life are more pronounced in medium GS.
5. DSA in LCF enhances the deformation inhomogeneity in medium and coarse grained conditions.
6. The LCF fracture mechanism is altered due to DSA; Brittle intergranular decohesion results from the occurrence of inhomogeneous plastic deformation.

REFERENCES

Abdel-Raouf, H., A. Plumtree and T.H. Topper (1973). ASTM, STP., 519., 28-57.

Bhanu Sankara Rao, K., M. Valsan., R. Sandhya., S.L. Mannan and P. Rodriguez (1986a). Grain size dependence of creep-fatigue-environment interaction in AISI 304 SS. In : Proc. Intl. Conf. on Creep, Tokyo, April 14-18, 1986, pp.77-83. JSME, Tokyo.

Bhanu Sankara Rao, K., M. Valsan., R. Sandhya., S.L. Mannan and P. Rodriguez (1986b). High Temperature Mateirals and Processes., 7, 171-177.

Bhanu Sankara Rao, K., H. Schiffers., H. Schuster and H. Nickel (1988a). Metall. Trans., 19A, 359-371.

Bhanu Sankara Rao, K. (1988b). Influence of metallurgical variables on LCF behaviour of type 304 stainless steel. Ph.D Thesis, Madras University, India.

Bressers, J. and B. Verhegghe (1981) Res. Mechanica Letters, 1, 55-59.

Coffin Jr, L.F. (1973). ASTM, STP., 520, 5-34.

Hua, G., E.R.D. Rios and K.J. Miller (1983). Fatigue of Engg. Mater. Struct., 6, 137-147.

Mughrabi, H., R. Wang., K.I. Differet and U. Essmann (1983). ASTM, STP., 811, 5-45.

Nilsson, J.O. and T. Thorvaldsson (1985). Fatigue & Fract. Engg. Mater. Struct., 8, 373-384.

Pelloux, R.M. and R.E. Stoltz (1976). Proc. Fourth Intl. Conf. on Strength of Metals and Alloys., Vol.3, pp.1023-1036.

Starke Jr, E.A. (1979). In : Fatigue and Microstructure, Proc. 1978 ASM Materials Science Seminar, pp.205-243, ASM, Metals Park, Ohio.

Wilson, D.A. and J.K. Tromans (1970). Acta Metall., 18, 1197-1208.

Yamaguchi, K., K. Kanazawa and S. Yoshida (1978). Mat. Sci. Engg., 33, 175-181.